

# Nitration and Inactivation of IDO by Peroxynitrite<sup>1</sup>

Hidetsugu Fujigaki,<sup>\*†</sup> Kuniaki Saito,<sup>2\*†</sup> Felix Lin,<sup>†</sup> Suwako Fujigaki,<sup>†</sup> Kanako Takahashi,<sup>\*</sup> Brian M. Martin,<sup>†</sup> Cai Y. Chen,<sup>†</sup> Junichi Masuda,<sup>\*†</sup> Jeffrey Kowalak,<sup>†</sup> Osamu Takikawa,<sup>‡</sup> Mitsuru Seishima,<sup>\*</sup> and Sanford P. Markey<sup>†</sup>

IDO induction can deplete L-tryptophan in target cells, an effect partially responsible for the antimicrobial activities and antiallogeneic T cell responses of IFN- $\gamma$  in human macrophages, dendritic cells, and bone marrow cells. L-Tryptophan depletion and NO production are both known to have an antimicrobial effect in macrophages, and the interaction of these two mechanisms is unclear. In this study we found that IDO activity was inhibited by the peroxynitrite generator, 3-(4-morpholinyl)sydnominine, in PMA-differentiated cytokine-induced THP-1 (acute monocytic leukemia) cells and IFN- $\gamma$ -stimulated PBMCs, whereas IDO protein expression was unaffected compared with that in untreated cells. Nitrotyrosine was detected in immunoprecipitated (IP)-IDO from PMA-differentiated cytokine-induced THP-1 cells treated with 3-(4-morpholinyl)sydnominine, but not from untreated cells. Treatment of IP-IDO and recombinant IDO (rIDO) with peroxynitrite significantly decreased enzyme activity. Nitrotyrosine was detected in both peroxynitrite-treated IP-IDO and rIDO, but not in either untreated IP-IDO or rIDO. Peptide analysis by liquid chromatography/electrospray ionization and tandem mass spectrometry demonstrated that Tyr<sup>15</sup>, Tyr<sup>345</sup>, and Tyr<sup>353</sup> in rIDO were nitrated by peroxynitrite. The levels of Tyr nitration and the inhibitory effect of peroxynitrite on IDO activity were significantly reduced in the Tyr<sup>15</sup>-to-Phe mutant. These results indicate that IDO is nitrated and inactivated by peroxynitrite and that nitration of Tyr<sup>15</sup> in IDO protein is the most important factor in the inactivation of IDO. *The Journal of Immunology*, 2006, 176: 372–379.

Indoleamine 2,3-dioxygenase is the rate-limiting and first enzyme of the L-tryptophan (L-Trp)<sup>3</sup>-kynurenine pathway that converts the essential amino acid L-Trp to N-formylkynurenine in mammalian extrahepatic tissues. IDO is induced by IFN- $\gamma$  in the course of an inflammatory response in many human cell types, including macrophages, astrocytes, fibroblasts, and epithelial cells. IDO induction can deplete L-Trp in target cells, and this effect is partially responsible for the antimicrobial, antiviral, and antiproliferative activities of IFN- $\gamma$  (1–4). These IDO-sensitive microorganisms are eukaryotic pathogens such as *Toxoplasma gondii*, prokaryotic pathogens such as *Chlamydia psittaci*, and bacteria such as group B streptococci and enterococci (5–8). L-Trp depletion is also involved in the inhibition of T cell proliferation by IFN- $\gamma$ -treated human monocyte-derived macrophages and dendritic cells (9–11). T cells are unable to proliferate in a Trp-depleted environment, and in vivo IDO activity in the mouse placenta protects allogeneic concepti from being rejected by a T cell-driven

mechanism (12, 13). It has been suggested that first-time activation of T cells in the absence of L-Trp may even result in the development of tolerance to the Ag presented (14–16). Furthermore, a recent study has suggested that the suppression of collagen-induced arthritis is caused by IDO-dependent mechanisms that suppress the Ag-specific CD4<sup>+</sup> T cells responsible for the development of rheumatoid arthritis (17). In that disease, specific cell populations (CD11c<sup>+</sup>CD8<sup>+</sup> T cells) produce large amounts of IFN- $\gamma$ , which, in turn, induces IDO and inducible NO synthase (iNOS) expression in CD11b<sup>+</sup> monocytes and CD11c<sup>+</sup> dendritic cells.

Several studies report that activation of L-arginine metabolism through iNOS induction leads to the formation of NO, which, in turn, down-regulates L-Trp metabolism by both directly inhibiting IDO activity as well as interfering with the induction of the enzyme (18–20). However, the inhibition of IDO by NO varies among species and tissues (21–23). The role of NO production by iNOS in human cells is complex, because NO produces cytostatic and cytotoxic effects. NO may react with superoxide, a product of the respiratory burst in macrophages, to form peroxynitrite, which itself is cytotoxic (24). NO and NO-derived reactive species produce chemical modifications that alter the structure and function of biomolecules. The NO-dependent nitration of protein Tyr residues to 3-nitrotyrosine increases during oxidative inflammatory conditions, resulting in a post-translational modification that reflects the extent of oxidant production under both physiological and pathological conditions (24). There has been increasing interest in the impact of Tyr nitration of protein and enzyme structure-function relationships in diverse clinical pathologies (25). These include changes in the catalytic activity of enzymes, cytoskeletal organization, and cell signal transduction.

Because of the importance of IDO to antimicrobial effects and inflammatory responses, we explored whether IDO is affected by peroxynitrite. We report for the first time the structural and functional consequences of the interaction between IDO and peroxynitrite.

\*Department of Informative Clinical Medicine, Gifu University Graduate School of Medicine, Gifu City, Japan; <sup>†</sup>Laboratory of Neurotoxicology, National Institute of Mental Health, Bethesda, MD 20892; and <sup>‡</sup>Department of Pharmacology, Hokkaido University, Sapporo, Japan

Received for publication January 20, 2005. Accepted for publication October 19, 2005.

The costs of publication of this article were defrayed in part by the payment of page charges. This article must therefore be hereby marked *advertisement* in accordance with 18 U.S.C. Section 1734 solely to indicate this fact.

<sup>1</sup> This work was supported in part by the Intramural Research Program of the National Institute of Mental Health, National Institutes of Health.

<sup>2</sup> Address correspondence and reprint requests to Dr. Kuniaki Saito, Department of Informative Clinical Medicine, Gifu University Graduate School of Medicine, 1-1 Yanagido, Gifu City, Gifu 501-1194, Japan. E-mail address: saito@cc.gifu-u.ac.jp

<sup>3</sup> Abbreviations used in this paper: L-Trp, L-tryptophan; DTPA, diethylenetriaminepenta-acetic acid; iNOS, inducible NO synthase; IP, immunoprecipitated; LC-MS/MS, liquid chromatography/electrospray ionization and tandem mass spectrometry; L-Kyn, L-kynurenine; SIN-1, 3-(4-morpholinyl)sydnominine; SNP, sodium nitroprusside dehydrate; Y15F, Tyr<sup>15</sup>-to-Phe mutant; Y345F, Tyr<sup>345</sup>-to-Phe mutant; Y353F, Tyr<sup>353</sup>-to-Phe mutant; rIDO, recombinant IDO.

## Materials and Methods

### Materials

Peroxyntirite and anti-nitrotyrosine Ab were purchased from Upstate Biotechnology. 3-(4-Morpholinyl)sydnonimine (SIN-1) was obtained from Dojindo Laboratories. The pGEX plasmid vector, PreScission protease, glutathione-Sepharose 4B, PD-10 column, membrane-blocking agent, peroxidase-labeled anti-mouse Ab, and ECL Plus Western Blotting Detection System were obtained from Amersham Biosciences. Anti-GAPDH mAb was purchased from Chemicon International. Diethylenetriaminepentaacetic acid (DTPA), formic acid, perchloric acid, sodium nitroprusside dehydrate (SNP; NO donor), PMA, and acetonitrile were purchased from Sigma-Aldrich. THP-1 cells were obtained from Health Science Research Resources Bank. Spin Concentrators 5000 Molecular Weight Cut-Off was purchased from Agilent Technologies. Endoproteinase Lys-C (sequencing grade) was obtained from Roche. Trypsin (sequencing grade) was purchased from Promega. HPLC grade acetonitrile was purchased from Burdick & Jackson. Human rIFN- $\gamma$  (sp. act.,  $2.0 \times 10^7$  U/mg), and TNF- $\alpha$  (sp. act.,  $1.0 \times 10^8$  U/mg) were purchased from BD Biosciences. LPS (from *Salmonella abortus equi*) was obtained from Sigma-Aldrich. All other chemicals of analytical grade were purchased from Sigma-Aldrich.

### Culture conditions

THP-1 cells were regularly cultivated in RPMI 1640 medium (Nikken Bio Medical Laboratory) supplemented with 10% (v/v) heat-inactivated FBS (Roche) and 100 U/ml penicillin-streptomycin (Invitrogen Life Technologies) and were maintained at 37°C in a humidified atmosphere of 95% air and 5% CO<sub>2</sub> as described previously (26). Human PBMCs from human volunteers were obtained from Advanced Biotechnologies. PBMCs were cultivated in DMEM supplemented with 10% FBS and harvested with trypsin-EDTA as described previously (26). For the SIN-1 treatment experiment, PBMCs were treated with 5 ng/ml IFN- $\gamma$  for 24 h, and the medium was replaced with IFN- $\gamma$  alone or IFN- $\gamma$  plus 500  $\mu$ M SIN-1, then incubated for an additional 24 h. Also, THP-1 cells were treated with 16 nM PMA for 48 h. At this time, the cells adhered to the bottom and exhibited macrophage-like morphology, and the cytokine mixture (5 ng/ml IFN- $\gamma$ , 10 ng/ml TNF- $\alpha$ , and 100 ng/ml LPS) was added to induce IDO. After 24 h, the medium was replaced with fresh medium containing cytokine mixture with 500  $\mu$ M SIN-1. For the SNP treatment experiment, PBMCs were treated with 5 ng/ml IFN- $\gamma$  alone or IFN- $\gamma$  plus 500 nM SNP for 24 h. After treatment, cells were washed with PBS and harvested with Cell Scraper in RIPA buffer containing 10 mM Tris-HCl, 1% Nonidet P-40, 150 mM NaCl, 1 mM EDTA, and 1 mM PMSF. Cell lysates were collected by centrifugation and used for immunoprecipitation, Western blotting, and IDO activity assay.

### Measurement of L-kynurenine (L-Kyn) in culture medium

L-Kyn concentrations in culture medium were measured by HPLC as described previously (27). First, culture medium was mixed with 2 vol of 3% perchloric acid. After centrifugation, the concentrations of L-Kyn in the supernatants were measured using HPLC with a 5-mm octyldecyl silane column (Eicom) and a spectrophotometric detector. UV signals were monitored at 355 nm. The mobile phase consisted of 1% of acetonitrile in 0.1 M sodium acetate (pH 3.9), and the flow rate was maintained at 0.75 ml/min throughout the chromatographic run.

### Measurement of nitrite and nitrate in culture medium

NO release in culture medium was determined spectrophotometrically by measuring the accumulation of nitrite and nitrate using the Nitrate/Nitrite Colorimetric Assay Kit (Cayman Chemical).

### Immunoprecipitation of IDO

Immunoprecipitation was performed using Dynabeads Protein G (Dyna Biotech) according to the manufacturer's instructions. Anti-human IDO Ab was cross-linked to Dynabeads Protein G with 20 mM dimethylpiperimidate in 0.2 M triethanolamine (pH 8.2). The cell lysate was added to the cross-linked beads and incubated overnight at 4°C. The protein-Ig Dynabeads Protein G complex was washed with 0.05% Tween 20 containing PBS, and protein was eluted with 0.1 M citrate (pH 2.0).

### Purification of recombinant IDO (rIDO)

A 1.2-kb full-length human IDO cDNA was ligated into a pGEX plasmid vector, and rIDO was expressed as a GST fusion protein in BL21 *Escherichia coli* in the presence of 7  $\mu$ M hemin. The recombinant fusion protein was purified from bacterial lysates by affinity chromatography using glutathione Sepharose 4B, and a GST fusion tag was removed by cleavage of

PreScission Protease. Before use, the purified rIDO was gel-filtered through a PD-10 column eluted with 100 mM potassium phosphate buffer (pH 7.4), and protein concentration was determined by the bicinchoninic acid protein assay (Pierce).

### Treatment of rIDO with peroxyntirite

rIDO was diluted in 50  $\mu$ l of potassium phosphate buffer containing 0.1 mM DTPA (pH 7.4), then treated with various concentrations of peroxyntirite for 15 min at room temperature while stirring. For decomposition of peroxyntirite, peroxyntirite was added to the buffer and incubated for 15 min before rIDO addition.

### Activity assay of IDO

IDO activity was determined by the methylene blue/ascorbate assay as previously described (27). The reaction mixture contained 50  $\mu$ l of rIDO or homogenate of THP-1 cells and 50  $\mu$ l of substrate solution. The composition of the substrate solution was 100 mM potassium phosphate buffer (pH 6.5), 50  $\mu$ M methylene blue, 20  $\mu$ g of catalase, 50 mM ascorbate, and 0.4 mM L-Trp. After incubation of the reaction mixture at 37°C, samples were acidified with 3% perchloric acid and centrifuged at 7000  $\times$  g for 10 min at 4°C. The concentrations of the enzymatic products were measured using HPLC. Enzyme activity was expressed as the product content per hour per milligram of protein.

### Western blot analysis

The samples were separated using NuPAGE 4–12% bis-Tris gels as recommended by the manufacturer (Invitrogen Life Technologies). Proteins were transferred to nitrocellulose membrane, blocked in PBS containing 0.05% Tween 20 (v/v) and 20% membrane blocking agent (w/v), and probed with anti-nitrotyrosine Ab (2  $\mu$ g/ml), anti-IDO Ab (0.5  $\mu$ g/ml), or anti-GAPDH Ab (1  $\mu$ g/ml). After overnight incubations with the primary Abs at 4°C, blots were washed and incubated with peroxidase-labeled anti-mouse Ab for 2 h at room temperature, and immunoreactive protein bands were visualized with the ECL system.

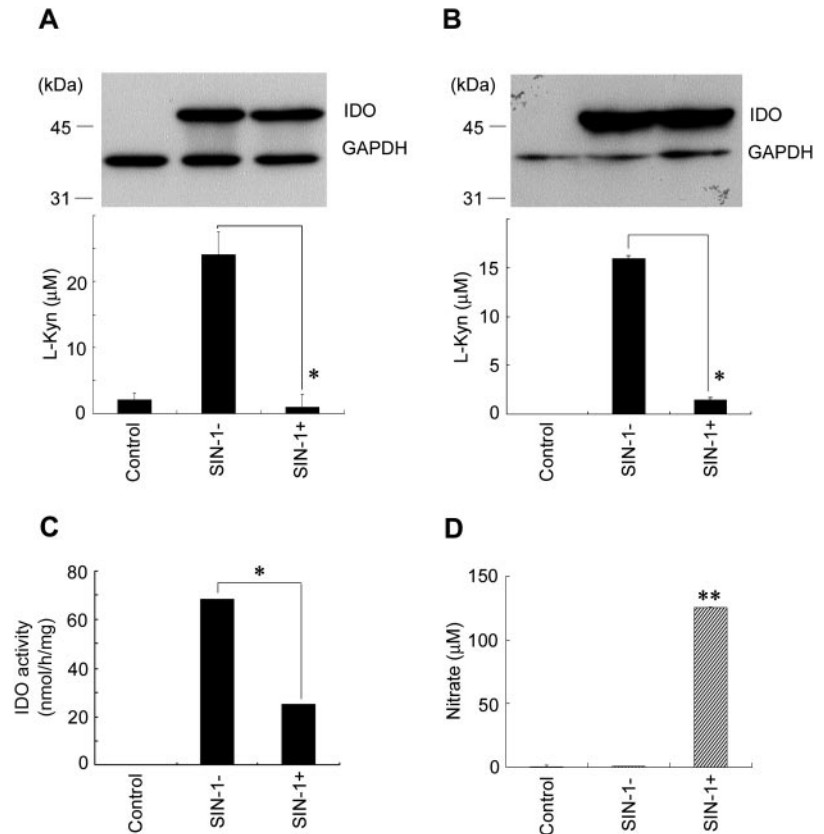
### Identification of nitrotyrosine residues in rIDO

After treatment with peroxyntirite, 50  $\mu$ g of rIDO was concentrated, and the buffer was exchanged with 0.1 M ammonium bicarbonate by 4-ml spin concentrators according to the manufacturer's instructions and evaporated to dryness using a centrifugal rotary evaporator. The protein was dissolved in the denaturation buffer containing 2 M urea and 2.25 mM DTT in ammonium bicarbonate and incubated for 15 min at 50°C to denature the protein. After denaturation, the protein was alkylated by addition of 100 mM iodoacetamide and incubated for 15 min at room temperature in the dark. After alkylation, 0.5  $\mu$ g of endoproteinase Lys-C was added to the protein, which was incubated for 15 h at 37°C, then 1  $\mu$ g of trypsin was added to the protein, which was incubated for 8 h at 37°C. The digested samples were evaporated in a centrifugal rotary evaporator, and dried digested samples were dissolved in 40  $\mu$ l of 5% acetonitrile and 0.1% formic acid (v/v). Two-dimensional liquid chromatography/tandem mass spectrometry (LC-MS/MS) analysis was conducted after tryptic digestion. The HPLC used was the LC-VP Series system consisting of a five-solvent delivery pump, an autosampler, and switching valves (all from Shimadzu) combined with a two-position low dead volume valve (Cheminert CN2; VICI Valco Instruments). Chromatographic separation was accomplished by loading peptide samples onto a Poly LC PolySulfoethyl A column (Poly LC) connected to a PicoFrit column (Thermo Hypersil-Keystone BetaBasic 18; New Objective). MS analysis was performed using PicoView nanospray ion source (New Objective) mounted on an LCQ (Thermo Electron) ion trap mass spectrometer (big-five scanning sequence data-dependant mode; mass range, 400–1800). Data analysis to identify nitrated peptides was performed using the Mascot sequence database-searching software (MatrixSciences). The MS/MS spectra of nitrated peptides were also examined by manual inspection to verify sites of nitration.

### Site-directed mutagenesis

Point mutations were introduced using the QuikChange site-directed mutagenesis kit (Stratagene). Oligonucleotides for generation of Tyr<sup>15</sup> (Y15F), Tyr<sup>345</sup> (Y345F), and Tyr<sup>353</sup> (Y353F) to the mutants (mutated residues are underlined) were as follows: 5'-CTGGACAATCAGTAAA GAGTTCATATTGATGAAGAAGTGG-3' and 5'-CCACTTCTTCAT CAATATGGAACTCTTTACTGATTGTCCAG-3' for Y15F; 5'-CTCCCT GAGGAGCTTCCATCTGCAAATCGTG-3' and 5'-CACGATTTGCA GATGGAAGGCTCCTCAGGGAG-3' for Y345F; and 5'-TGCAAATCG TGACTAAGTTCATCCTGATTCTGCAAG-3' and 5'-CTTGACAGGA

**FIGURE 1.** Effects of SIN-1 on IDO protein content and IDO activity in cytokine-treated THP-1 or PBMCs. PBMCs were treated with 5 ng/ml IFN- $\gamma$  for 24 h, and the medium was replaced with fresh medium containing IFN- $\gamma$  (SIN-1<sup>-</sup>) or IFN- $\gamma$  plus SIN-1 (SIN-1<sup>+</sup>) and incubated for 24 h. After the treatment, culture media and cell extracts were collected, IDO protein and GAPDH were detected by Western blotting (A, upper panel), and L-Kyn concentrations were determined in the culture medium (A, lower panel) were measured. THP-1 cells were stimulated for 48 h with PMA (16 nM), and the medium was replaced with fresh medium containing a cytokine mixture. After 24 h, the medium was replaced with fresh medium containing cytokine mixture alone (SIN-1<sup>-</sup>) or cytokine mixture plus SIN-1 (SIN-1<sup>+</sup>) and incubated for 24 h. IDO protein and GAPDH were detected by Western blotting (B, upper panel), and L-Kyn concentrations were determined in the culture medium (B, lower panel) were measured. At the same time, IDO activity in the THP-1 cell lysate (C) and the total concentration of nitrate plus nitrite in culture medium (D) were measured. Western blotting was repeated five times and produced the same results. The results of IDO activity, L-Kyn, and nitrate are the mean  $\pm$  SD of five independent experiments conducted in duplicate. \*,  $p < 0.001$  compared with SIN-1<sup>-</sup>; \*\*,  $p < 0.001$  compared with control.



ATCAGGATGAACTTAGTCACGATTGCA-3' for Y353F. The double- and triple-Tyr mutants (Y15/345F, Y15/353F, Y345/353F, and Y15/345/353F) were also created. Each mutagenesis of rIDO was confirmed by DNA sequence analysis with an ABI PRISM 3100 automatic sequencer (Applied Biosystems). All rIDO mutants were also purified as described above.

#### Statistics

Intrasample difference was assessed using paired Student's *t* test. Differences were considered significant at  $p < 0.05$ . All results are shown as the mean  $\pm$  SD.

## Results

### Inactivation of IDO activity and nitration of IDO protein by SIN-1 in cytokine-treated cells

Human PBMCs stimulated with IFN- $\gamma$  produced significantly higher amounts of IDO protein and L-Kyn concentrations in culture medium compared with the controls (Fig. 1A). Although IDO protein levels were unchanged between IFN- $\gamma$ -treated and IFN- $\gamma$  plus SIN-1-treated cells, the L-Kyn concentration was significantly decreased in IFN- $\gamma$ - plus 500  $\mu$ M SIN-1-treated human PBMCs compared with IFN- $\gamma$ -treated cells. Similarly, differentiated THP-1 cells stimulated with PMA and cytokines (IFN- $\gamma$ , TNF- $\alpha$ , and LPS) produced significantly higher amounts of IDO protein and L-Kyn concentration in culture medium compared with controls. The L-Kyn concentration in culture medium and IDO activity in cell lysate were significantly decreased in SIN-1-treated THP-1 cells, although the IDO protein expression level was not different between SIN-1-treated and untreated cells (Fig. 1, B and C). In contrast, the nitrate concentration was significantly increased in SIN-1-treated THP-1 cells (Fig. 1D). In addition, we found that the L-Kyn concentration was significantly decreased in IFN- $\gamma$  plus 500 nM SNP (NO donor)-treated PBMCs compared with IFN- $\gamma$ -treated cells, although IDO protein levels were unchanged between IFN- $\gamma$ -treated and IFN- $\gamma$  plus SNP-treated cells (data not shown).

To determine whether IDO is nitrated in SIN-1-treated cells, IDO from PMA-differentiated cytokine-induced THP-1 cells with or without SIN-1 was purified by immunoprecipitation. Western blot analysis using anti-nitrotyrosine Ab was used for the detection of nitrotyrosine in immunoprecipitated (IP)-IDO. Nitrotyrosine was detected in IP-IDO from PMA-differentiated cytokine-induced THP-1 cells with SIN-1, but not in untreated cells (Fig. 2). These results indicate that SIN-1 decreased IDO activity without decreasing IDO protein expression levels, and that IDO protein is nitrated in SIN-1-treated cells.

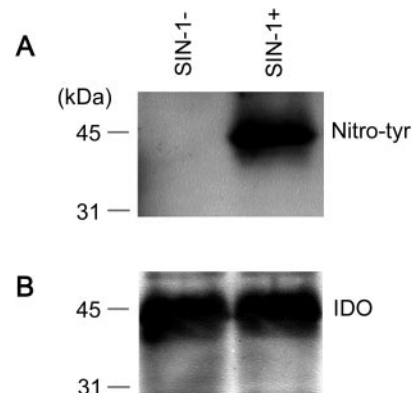


**FIGURE 2.** Nitration of IDO in PMA-differentiated, cytokine-induced THP-1 cells treated with SIN-1. PMA-differentiated, cytokine-induced THP-1 cells were treated for 24 h with cytokine mixture alone (SIN-1<sup>-</sup>) or cytokine mixture plus SIN-1 (SIN-1<sup>+</sup>) as described in *Materials and Methods*. IDO was purified from the control and SIN-1-treated THP-1 cells using immunoprecipitation with anti-IDO Ab. Purified IDO was probed with anti-nitrotyrosine (A) and anti-IDO (B) Abs. These experiments were repeated three times and produced the same results.

### Inactivation and nitration of IP-IDO and rIDO by peroxynitrite

We analyzed IP-IDO from PMA-differentiated cytokine-induced THP-1 cells and rIDO by IDO activity assay and Western blot analysis using anti-nitrotyrosine Ab and anti-IDO Ab after exposure to peroxynitrite. Enzyme activity in IP-IDO and rIDO was significantly decreased by the addition of peroxynitrite (Fig. 3A). IDO protein levels were unaffected (Fig. 3B), and nitrotyrosine was detected in both peroxynitrite-treated IP-IDO and rIDO, but was not detected in either untreated IP-IDO or rIDO (Fig. 3C). The addition of increasing amounts of peroxynitrite to rIDO resulted in increased nitrotyrosine levels and inhibition of IDO activity in a dose-dependent manner, with the IDO protein concentration remaining constant (Fig. 4). It is of note that decomposed peroxynitrite had no effect on IDO activity or levels of nitrotyrosine in rIDO (Fig. 4, lane d). These results indicate that IDO is nitrated and inactivated by peroxynitrite.

### Identification of nitrated residues

To determine which Tyr residues in the rIDO were nitrated, peroxynitrite-treated or untreated rIDO was digested with endoproteinase Lys-C and trypsin, and peptides were separated by LC-MS/MS. The amino acid sequence coverage obtained by LC-MS/MS analysis of the LysC and tryptic digests of peroxynitrite-treated rIDO is indicated in Fig. 5A (81.14%). All peptides, including Tyr residues, were covered. Assignments of nitration sites were verified by manual inspection of the tandem mass spectra. The results indicated the presence of three nitrated peptides in the peroxynitrite-treated rIDO digests and

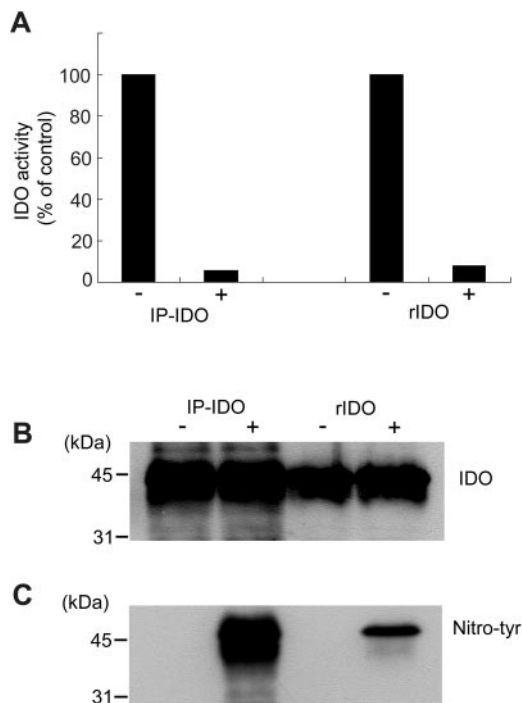


**FIGURE 3.** Effects of peroxynitrite on IDO activity and nitrotyrosine levels in IP-IDO and rIDO. Immunoprecipitation was performed as described in *Materials and Methods*. IP-IDO and rIDO were incubated without (-) or with (+) 100  $\mu$ M peroxynitrite in 100 mM potassium phosphate buffer (pH 7.4), containing 100 mM DTPA for 15 min at room temperature. Samples were subjected to determinations of IDO catalytic activity (A) and immunoblotting with an Ab against IDO (B) or nitrotyrosine (C). These experiments were repeated three times and produced the same results. Data for IDO activity in A are expressed as a percentage of each untreated control value.

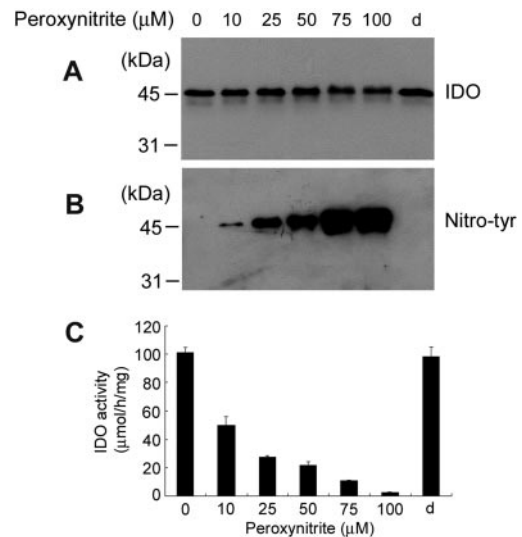


**FIGURE 4.** Effects of increasing concentrations of peroxynitrite on nitrotyrosine levels and IDO activity in rIDO. rIDO was treated with the indicated concentrations of peroxynitrite or 1 mM decomposed peroxynitrite (lane d) in 100 mM potassium phosphate buffer (pH 7.4) containing 100 mM DTPA for 30 min at room temperature. Samples were subjected to immunoblotting with an Ab against IDO (A), immunoblotting with an Ab against nitrotyrosine (B), or determination of IDO catalytic activity (C). These experiments were repeated five times and produced the same results. Data for IDO activity in C represent the mean  $\pm$  SD of four to six independent experiments conducted in duplicate.

established the nitration of Tyr<sup>15</sup>, Tyr<sup>345</sup>, and Tyr<sup>353</sup> residues (Fig. 5, B–D). None of nitration-related peptides was seen in untreated rIDO.

### Site-directed mutagenesis of Tyr residues

To investigate which Tyr residue has the most important role in nitration and inactivation of IDO, Tyr<sup>15</sup>, Tyr<sup>345</sup>, and Tyr<sup>353</sup> residues in rIDO were mutated to Phe, and the effects of peroxynitrite on Tyr nitration and enzyme activity expressed by each mutant were measured. The effect of Tyr mutation on basal IDO activity is shown in Table I. All Tyr-to-Phe mutants of rIDO retained catalytic activity, but some were sensitive to substitution. The conservative substitution of Tyr<sup>15</sup>, Tyr<sup>345</sup>, and Tyr<sup>353</sup> with Phe had only minor impact on IDO activity ( $\sim$ 79 to  $\sim$ 109%), but double and triple mutants were significantly less effective than the wild type ( $\sim$ 15 to  $\sim$ 38%). These data suggest that the double and triple mutants are not comparable for the effect of peroxynitrite with wild-type IDO. Thus, we determined the effect of peroxynitrite on Tyr nitration and enzyme activity in the single mutants. Fig. 6B shows the levels of nitrotyrosine in each rIDO as assessed by anti-nitrotyrosine immunoreactivity. The levels of nitrotyrosine in peroxynitrite-treated Y15F mutant were significantly reduced compared with those of wild-type rIDO. In addition, inhibition of enzyme activity by 10  $\mu$ M peroxynitrite in the wild type was  $\sim$ 68%, although inhibition of enzyme activity in the Y15F mutant was only  $\sim$ 35% (Fig. 6C). These results indicate that nitration of Tyr<sup>15</sup> in IDO protein is most responsible for the inactivation of IDO.

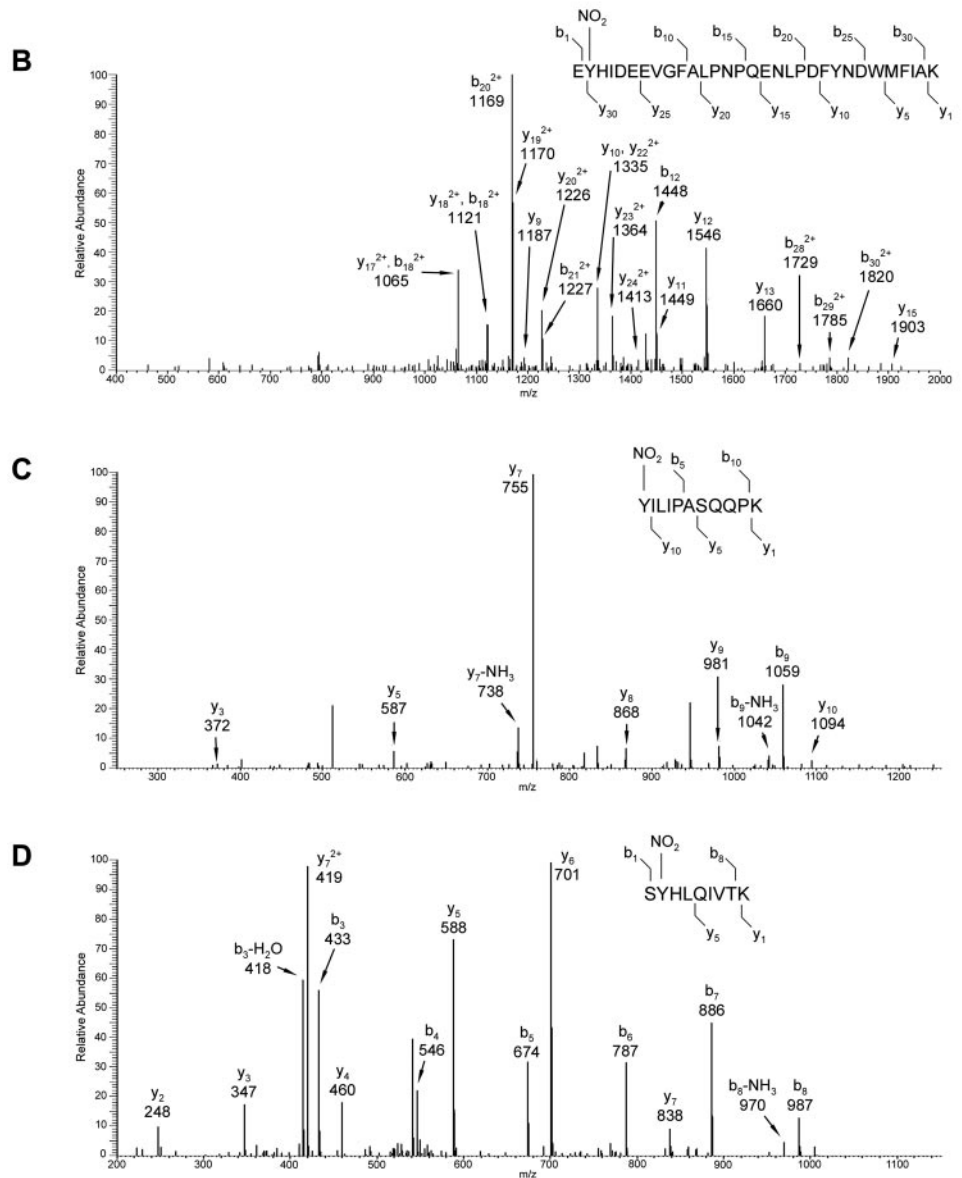
### Discussion

This study clearly demonstrates for the first time that IDO is nitrated by peroxynitrite, resulting in inhibition of enzyme activity. It is thought that peroxynitrite is produced by inflammatory cells to defend against cancer cells or infection caused by parasites, viruses, and bacteria. At the same time, peroxynitrate can damage

A

1 MAHAMENSWT ISKEYHIDEE<sup>\*</sup> VGFALPNPQE NLPDFYNDWM FIAKHLPLDI ESGQLRERVE  
 61 KLNMLSIDHL TDHKSQRLAR LVLGCITMAY VWGKGHDVVR KVLPRNIAVP YCQLSKKLEL  
 121 PPILVYADCV LANWKKKDPN KPLTYENMDV LFSFRDGDSCS KGFFLVSLLV EIAAASAIKV  
 181 IPTVFKAMQM QERDTLLKAL LEIASCLEKA LQVFHQIHDH VNPKAFFSVL RIYLSGWKGN  
 241 PQLSDGLVYE GFWEDPKEFA GGSAGQSSVF QCFDVLGGIQ QTAGGGHAAQ FLQDMRRYMP  
 301 PAHRNFLCSL ESNPSVREFV LSKGDAGLRE AYDACVKALV SLRSYHLQIV<sup>\*</sup> TKYILIPASQ<sup>\*</sup>  
 361 QPKENKTSED PSKLEAKGTG GTDLMNFLKT VRSTTEKSL L KEG

**FIGURE 5.** Amino acid sequence coverage and sites of nitration obtained by LC-MS/MS analysis of peroxynitrite-treated rIDO. IDO was nitrated with peroxynitrite as described in *Materials and Methods* and subjected to endoprotease Lys-C and trypsin digestion, and peptides were separated on a reverse phase HPLC column on-line with an electrospray ionization, ion trap mass spectrometer. The amino acid sequence coverage obtained by LC-MS/MS is indicated in bold. The verified nitrated peptide regions are underlined, and asterisks designate nitrotyrosine residues (A). B–D, Annotated mass spectra of peptides containing nitrotyrosine observed after the reaction of peroxynitrate with rIDO. Collisionally induced fragmentation spectrum of  $m/z$  1263.2 ( $MH^{3+}$ ) in B corresponds to the amino acid sequence EY(NO<sub>2</sub>)HIDEEVGFALPNPQENLPDFYNDWMFIAK; that of  $m/z$  1302 ( $MH^+$ ) in C corresponds to the amino acid sequence Y(NO<sub>2</sub>)ILIPASQQK; that of  $m/z$  567 ( $MH^{2+}$ ) in D corresponds to the amino acid sequence SY(NO<sub>2</sub>)HLQIVTK. Type b ions contain the N-terminal portion of the peptide; type y ions contain the C-terminal portion.



host cells and tissues (28). Nitration of Tyr residues in proteins is a post-translational modification associated with oxidative stress and activation of NO. Activated macrophages, for example, can simultaneously generate large fluxes of NO and superoxide, neither of which is unusually reactive (25). These two substances,

however, rapidly combine to produce the far more reactive peroxynitrite anion with an extensive range of physiological consequences, including lipid oxidation, DNA damage, and protein modification via formation of 3-nitrotyrosine (24). Protein nitration has been observed in connection with >60 human disorders,

Table I. Effect of tyrosine mutation on basal IDO activity

Tyrosine Mutant	IDO Activity ( $\mu\text{mol/h/mg}$ ) <sup>a</sup>	% of Wild Type (%) <sup>b</sup>
Wild type	4.91 $\pm$ 0.09	100
Y15F	5.37 $\pm$ 0.12	109.15 $\pm$ 2.42
Y345F	4.50 $\pm$ 0.19	91.55 $\pm$ 3.87
Y353F	3.91 $\pm$ 0.08	79.57 $\pm$ 3.87
Y15/345F	1.42 $\pm$ 0.06	28.80 $\pm$ 1.15 <sup>c</sup>
Y15/353F	0.75 $\pm$ 0.07	15.30 $\pm$ 3.80 <sup>c</sup>
Y345/353F	1.88 $\pm$ 0.19	38.21 $\pm$ 3.80 <sup>c</sup>
Y15/345/353F	1.03 $\pm$ 0.07	20.95 $\pm$ 3.56 <sup>c</sup>

<sup>a</sup> IDO activity represents the mean  $\pm$  SD for three to five experiments performed in duplicate.

<sup>b</sup> IDO activity is expressed as a percentage of the wild type and represents the means  $\pm$  SD.

<sup>c</sup> Significantly different from the wild-type group;  $p < 0.001$ .

and there has been increasing interest in the impact of Tyr nitration on protein and enzyme structure-function relationships in diverse clinical pathologies, including neurodegenerative diseases, acute lung injury, atherosclerosis, bacterial and viral infection, and chronic inflammation (29–32). Thus, an understanding of both the mechanisms underlying protein nitration and the impact of this post-translational protein modification on cell and organ functions will provide insight into the pathogenic mechanisms of inflammatory diseases and novel therapeutic strategies for limiting tissue inflammatory injury (25, 33).

L-Trp depletion and NO production are both known to have an antimicrobial effect, and the interaction of these two events is still under investigation. It was previously thought that these two events were species specific, with the microbicidal activity of NO restricted to rodent cells and the IDO-mediated Trp depletion occurring only in humans (18, 21). Recently, it has become clear that both events occur in humans, resulting in a more complex interaction (5, 23, 34). It has been suggested that NO donors inhibit IDO activity in IFN- $\gamma$ -treated human PBMCs (18). A recent study suggests that endogenous and exogenous NOs strongly reduce the IDO protein content in IFN- $\gamma$ - and IL-1 $\beta$ -treated RT4 cells, which expresses both IDO activity and strong iNOS activity, and that this effect depends not on transcriptional, but on post-translational, reg-

ulation resulting from accelerated proteasomal degradation of IDO (20).

However, we demonstrated that IDO activity was significantly reduced in SIN-1-treated PBMCs and THP-1 cells, although IDO protein levels were not different between cytokine-treated and cytokine- plus SIN-1-treated PMA-differentiated THP-1 cells. It is known that SIN-1 can easily penetrate cells and generate peroxynitrite in cell culture systems (35). A recent study demonstrated that the concentration of peroxynitrite in cell culture systems was linearly dependent upon the SIN-1 concentration, and that the maximum concentration of peroxynitrite was very low, ranging from 1.2 to 3.6% of added SIN-1 (36). These studies support the concept that peroxynitrite affects intracellular IDO in SIN-1-treated cells, and in this study we have demonstrated that IP-IDO from SIN-1-treated THP-1 cells is nitrated (Fig. 2). NO adducts of IDO are believed to be involved in modulation of the catalytic activity of this heme protein (37), but no such evidence has been indicated in cell culture systems or in vivo. Much of NO-mediated pathogenicity depends on the formation of peroxynitrite, which is typically more reactive and toxic than NO (24). We also found that the L-Kyn concentration was significantly decreased in IFN- $\gamma$ - plus 500 nM SNP-treated PBMCs compared with that in IFN- $\gamma$ -treated cells, although IDO protein levels were unchanged between IFN- $\gamma$ -treated and IFN- $\gamma$ - plus SNP-treated cells. It is possible that peroxynitrite derived from SNP affects intracellular IDO in SNP-treated PBMCs, because NO released from SNP is able to react with superoxide anions, resulting in the formation of peroxynitrite in cell culture systems (38, 39). However, the present results demonstrate that a 1000 times lower concentration of SNP (500 nM) inhibited IDO activity to the same extent as SIN-1 (500  $\mu\text{M}$ ) in IFN- $\gamma$ -stimulated PBMCs. It is likely that NO is more efficient than peroxynitrite in inhibiting IDO activity in SNP-treated PBMCs. Additional studies are required to clarify this issue.

A schematic diagram illustrating the interaction between IDO and peroxynitrite is shown in Fig. 7. Enzymatically, IDO initiates the degradation of tryptophan. Functionally, IDO has been demonstrated to be very important in maintaining maternal tolerance (40), and it has been proposed that NO may also play a role in maternal tolerance toward the fetus (41). It is known that peroxynitrite, which is produced by monocyte/macrophage lineage or

**FIGURE 6.** Effects of peroxynitrite on nitrotyrosine levels and IDO activity in each mutant IDO. Wild-type IDO and Y15F, Y345F, or Y353F mutants were treated with the indicated concentrations of peroxynitrite as described in *Materials and Methods* and subjected to immunoblotting with an Ab against IDO (A) and nitrotyrosine (B). Peroxynitrite (100  $\mu\text{M}$ ) that had been decomposed before use was noneffective on levels of IDO and nitrotyrosine in each rIDO (lane d). These experiments were repeated four times and produced the same results. Wild-type and each mutant IDO were treated with 10  $\mu\text{M}$  peroxynitrite and subjected to IDO activity assay (C). IDO activity is expressed as a percentage of the untreated control value for each mutant. Results represent the mean  $\pm$  SD of four to six independent experiments conducted in duplicate. \*, Significantly different from the wild-type group at  $p < 0.001$ .

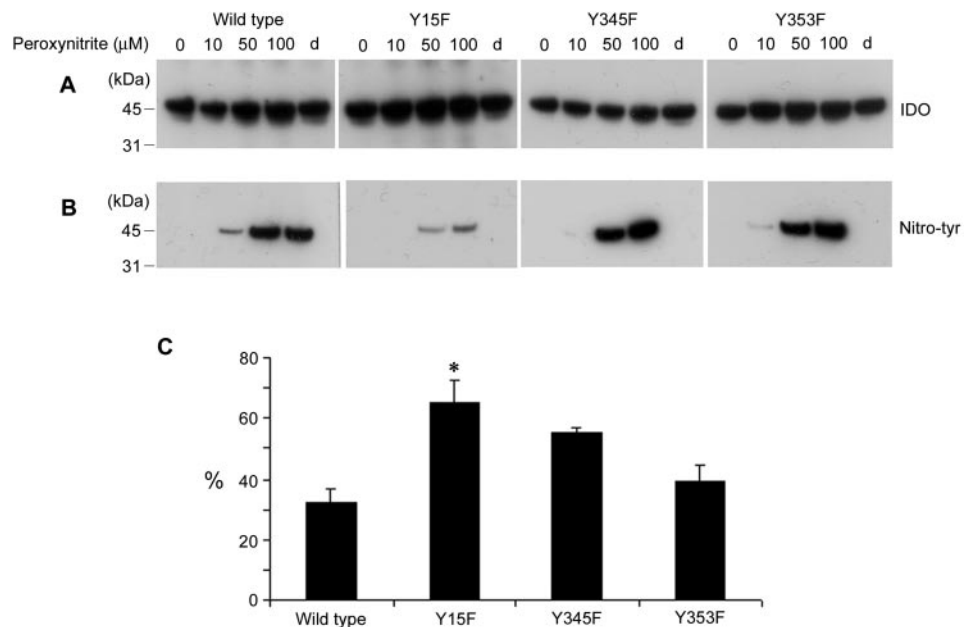
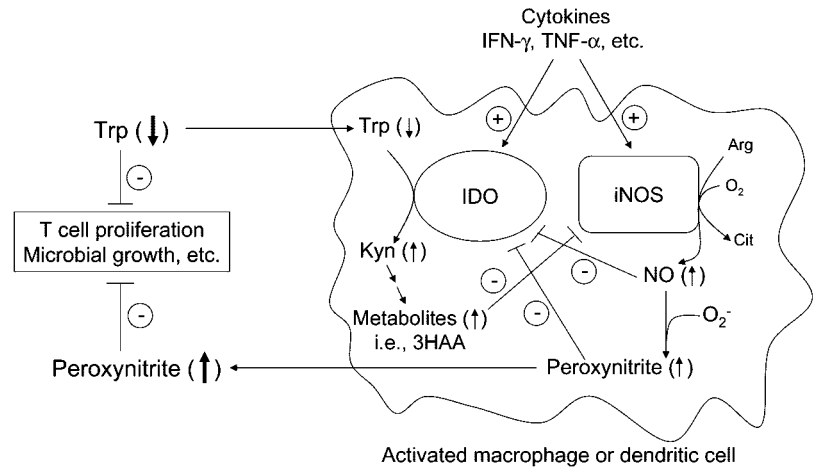


**FIGURE 7.** Schematic overview of the interaction between IDO and peroxynitrite. Both IDO and iNOS were stimulated by several proinflammatory cytokines in macrophages or dendritic cells, and they may play a role in tolerance and antimicrobial growth. NO inhibits IDO activity, and peroxynitrite inhibits IDO activity by nitration of IDO. Additionally, metabolites derived from L-Trp degradation via the IDO pathway can interfere with iNOS (see *Discussion*). Arg, arginine; Cit, citrulline; 3HAA, 3-hydroxyantranilic acid.



Gr-1<sup>+</sup> dendritic cells, is a powerful oxidant that can inhibit T cell activation and proliferation by impairment of Tyr phosphorylation and apoptotic death (42) or through a CD3/CD28 costimulation mechanism (43). There is a possible mechanism of interaction between IDO and peroxynitrite for the inhibition of T cell proliferation. NO inhibits IDO activity by binding to the heme of IDO (18), and peroxynitrite also inhibits IDO activity by nitration of IDO. Metabolites derived from L-Trp degradation via the IDO pathway can also interfere with iNOS activity or expression. For example, 3-hydroxyantranilic acid can inhibit iNOS mRNA expression and enzymatic activity induced by IFN (22). Both IDO and iNOS may play a role in tolerance, but elaborating these mechanisms requires additional experimental evidence.

Fig. 6 shows that nitration of Tyr<sup>15</sup> in IDO protein is most responsible for the inactivation of IDO by peroxynitrite. The IDO activity of Y15F mutant treated with 10  $\mu$ M peroxynitrite was ~30% higher than that of the wild type treated with the same concentration of peroxynitrite. Table I shows that Y15F mutant expresses wild-type levels of basal IDO activity, and the activities of Y345F and Y353F are ~10 and ~20% lower than those in the wild type, respectively. These data indicate that substitution of Tyr<sup>15</sup>, Tyr<sup>345</sup>, and Tyr<sup>353</sup> with Phe had only a minor impact on IDO activity in the single mutants. However, the double and triple mutants expressed much lower levels of basal IDO activity (15–38% of wild type). Although all double and triple mutants were much less inhibited by 10  $\mu$ M peroxynitrite than the wild type cells treated with the same concentration of peroxynitrite (10–20% higher than wild type), the inhibition ratio was higher than that for Y15F mutant. Furthermore, even though the basal levels of activity and the inhibition ratio were different between mutants, all Tyr mutants of rIDO were almost completely inhibited by 1 mM peroxynitrite (data not shown). Taken together, these data indicate that Tyr nitration is not exclusively the mode of IDO inhibition by peroxynitrite. Several studies have suggested that the inhibition of enzyme activity (e.g., Tyr hydroxylase and tryptophan hydroxylase) by peroxynitrite is caused by oxidation of cysteine residues or sulfhydryl oxidation instead of Tyr nitration (44, 45). There is a possibility that IDO may be affected by such modifications. However, the concentration of peroxynitrite in the physiological state is very low, and peroxynitrite is estimated to have a very short half-life (<20 ms) (25). Our study suggests that the inhibition of IDO activity by low concentrations of peroxynitrite may be caused mainly by nitration of Tyr<sup>15</sup>. Furthermore, considering the basal activity of each mutant, the possibility exists that the tertiary structure of each double- and triple-mutant IDO may be altered.

The present results demonstrate that IDO is nitrated and inactivated by peroxynitrite, and identify Tyr<sup>15</sup>, Tyr<sup>345</sup>, and Tyr<sup>353</sup> in IDO as the sites of nitration. Furthermore, nitration of Tyr<sup>15</sup> is the most responsible for inactivation of IDO by peroxynitrite.

## Acknowledgments

We thank John Cole for proofreading the English of this manuscript.

## Disclosures

The authors have no financial conflict of interest.

## References

- Gupta, S. L., J. M. Carlin, P. Pyati, W. Dai, E. R. Pfefferkorn, and M. J. Murphy, Jr. 1994. Antiparasitic and antiproliferative effects of indoleamine 2,3-dioxygenase enzyme expression in human fibroblasts. *Infect. Immun.* 62: 2277–2284.
- Sarkhosh, K., E. E. Tredget, A. Karami, H. Uludag, T. Iwashina, R. T. Kilani, and A. Ghahary. 2003. Immune cell proliferation is suppressed by the interferon- $\gamma$ -induced indoleamine 2,3-dioxygenase expression of fibroblasts populated in collagen gel (FPCG). *J. Cell Biochem.* 90: 206–217.
- Mackler, A. M., E. M. Barber, O. Takikawa, and J. W. Pollard. 2003. Indoleamine 2,3-dioxygenase is regulated by IFN- $\gamma$  in the mouse placenta during *Listeria monocytogenes* infection. *J. Immunol.* 170: 823–830.
- Meisel, R., A. Zibert, M. Laryea, U. Gobel, W. Daubener, and D. Dilloo. 2004. Human bone marrow stromal cells inhibit allogeneic T-cell responses by indoleamine 2,3-dioxygenase-mediated tryptophan degradation. *Blood* 103: 4619–4621.
- Fujigaki, S., K. Saito, M. Takemura, N. Maekawa, Y. Yamada, H. Wada, and M. Seishima. 2002. L-Tryptophan-L-kynurenine pathway metabolism accelerated by *Toxoplasma gondii* infection is abolished in  $\gamma$  interferon-gene-deficient mice: cross-regulation between inducible nitric oxide synthase and indoleamine-2,3-dioxygenase. *Infect. Immun.* 70: 779–786.
- Rottenberg, M. E., A. Gigliotti Rothfuchs, D. Gigliotti, M. Ceausu, C. Une, V. Levitsky, and H. Wigzell. 2000. Regulation and role of IFN- $\gamma$  in the innate resistance to infection with *Chlamydia pneumoniae*. *J. Immunol.* 164: 4812–4818.
- Currier, A. R., M. H. Ziegler, M. M. Riley, T. A. Babcock, V. P. Telbis, and J. M. Carlin. 2000. Tumor necrosis factor- $\alpha$  and lipopolysaccharide enhance interferon-induced antichlamydial indoleamine dioxygenase activity independently. *J. Interferon Cytokine Res.* 20: 369–376.
- MacKenzie, C. R., R. Langen, O. Takikawa, and W. Daubener. 1999. Inhibition of indoleamine 2,3-dioxygenase in human macrophages inhibits interferon- $\gamma$ -induced bacteriostasis but does not abrogate toxoplasmatosis. *Eur. J. Immunol.* 29: 3254–3261.
- Mellor, A. L., D. B. Keskin, T. Johnson, P. Chandler, and D. H. Munn. 2002. Cells expressing indoleamine 2,3-dioxygenase inhibit T cell responses. *J. Immunol.* 168: 3771–3776.
- Frumento, G., R. Rotondo, M. Tonetti, and G. B. Ferrara. 2001. T cell proliferation is blocked by indoleamine 2,3-dioxygenase. *Transplant. Proc.* 33: 428–430.
- Munn, D. H., E. Shafizadeh, J. T. Attwood, I. Bondarev, A. Pashine, and A. L. Mellor. 1999. Inhibition of T cell proliferation by macrophage tryptophan catabolism. *J. Exp. Med.* 189: 1363–1372.
- Mellor, A. L., and D. H. Munn. 1999. Tryptophan catabolism and T-cell tolerance: immunosuppression by starvation? *Immunol. Today* 20: 469–473.
- Mellor, A. L., P. Chandler, G. K. Lee, T. Johnson, D. B. Keskin, J. Lee, and D. H. Munn. 2002. Indoleamine 2,3-dioxygenase, immunosuppression and pregnancy. *J. Reprod. Immunol.* 57: 143–150.

14. Friberg, M., R. Jennings, M. Alsarraj, S. Dessureault, A. Cantor, M. Extermann, A. L. Mellor, D. H. Munn, and S. J. Antonia. 2002. Indoleamine 2,3-dioxygenase contributes to tumor cell evasion of T cell-mediated rejection. *Int. J. Cancer* 101: 151–155.
15. Uytendove, C., L. Pilotte, I. Theate, V. Stroobant, D. Colau, N. Parmentier, T. Boon, and B. J. Van den Eynde. 2003. Evidence for a tumoral immune resistance mechanism based on tryptophan degradation by indoleamine 2,3-dioxygenase. *Nat. Med.* 9: 1269–1274.
16. Travers, M. T., I. F. Gow, M. C. Barber, J. Thomson, and D. B. Shennan. 2004. Indoleamine 2,3-dioxygenase activity and L-tryptophan transport in human breast cancer cells. *Biochim. Biophys. Acta* 1661: 106–112.
17. Seo, S. K., J. H. Choi, Y. H. Kim, W. J. Kang, H. Y. Park, J. H. Suh, B. K. Choi, D. S. Vinay, and B. S. Kwon. 2004. 4-1BB-mediated immunotherapy of rheumatoid arthritis. *Nat. Med.* 10: 1088–1094.
18. Thomas, S. R., D. Mohr, and R. Stocker. 1994. Nitric oxide inhibits indoleamine 2,3-dioxygenase activity in interferon- $\gamma$  primed mononuclear phagocytes. *J. Biol. Chem.* 269: 14457–14464.
19. Daubener, W., C. Hucke, K. Seidel, U. Hadding, and C. R. MacKenzie. 1999. Interleukin-1 inhibits  $\gamma$  interferon-induced bacteriostasis in human uroepithelial cells. *Infect. Immun.* 67: 5615–5620.
20. Hucke, C., C. R. MacKenzie, K. D. Adjogbe, O. Takikawa, and W. Daubener. 2004. Nitric oxide-mediated regulation of  $\gamma$  interferon-induced bacteriostasis: inhibition and degradation of human indoleamine 2,3-dioxygenase. *Infect. Immun.* 72: 2723–2730.
21. Alberati-Giani, D., P. Malherbe, P. Ricciardi-Castagnoli, C. Kohler, S. Denis-Donini, and A. M. Cesura. 1997. Differential regulation of indoleamine 2,3-dioxygenase expression by nitric oxide and inflammatory mediators in IFN- $\gamma$ -activated murine macrophages and microglial cells. *J. Immunol.* 159: 419–426.
22. Sekkai, D., O. Guittet, G. Lemaire, J. P. Tenu, and M. Lepoivre. 1997. Inhibition of nitric oxide synthase expression and activity in macrophages by 3-hydroxyanthranilic acid, a tryptophan metabolite. *Arch. Biochem. Biophys.* 340: 117–123.
23. Alberati-Giani, D., and A. M. Cesura. 1998. Expression of the kynurenine enzymes in macrophages and microglial cells: regulation by immune modulators. *Amino Acids* 14: 251–255.
24. Radi, R. 2004. Nitric oxide, oxidants, and protein tyrosine nitration. *Proc. Natl. Acad. Sci. USA* 101: 4003–4008.
25. Schopfer, F. J., P. R. Baker, and B. A. Freeman. 2003. NO-dependent protein nitration: a cell signaling event or an oxidative inflammatory response? *Trends Biochem. Sci.* 28: 646–654.
26. Heyes, M. P., C. Y. Chen, E. O. Major, and K. Saito. 1997. Different kynurenine pathway enzymes limit quinolinic acid formation by various human cell types. *Biochem. J.* 326: 351–356.
27. Fujigaki, S., K. Saito, K. Sekikawa, S. Tone, O. Takikawa, H. Fujii, H. Wada, A. Noma, and M. Seishima. 2001. Lipopolysaccharide induction of indoleamine 2,3-dioxygenase is mediated dominantly by an IFN- $\gamma$ -independent mechanism. *Eur. J. Immunol.* 31: 2313–2318.
28. Beckman, J. S., and W. H. Koppenol. 1996. Nitric oxide, superoxide, and peroxynitrite: the good, the bad, and ugly. *Am. J. Physiol.* 271: C1424–C1437.
29. Kuhn, D. M., S. A. Sakowski, M. Sadidi, and T. J. Geddes. 2004. Nitrotyrosine as a marker for peroxynitrite-induced neurotoxicity: the beginning or the end of the end of dopamine neurons? *J. Neurochem.* 89: 529–536.
30. Hall, E. D., M. R. Detloff, K. Johnson, and N. C. Kupina. 2004. Peroxynitrite-mediated protein nitration and lipid peroxidation in a mouse model of traumatic brain injury. *J. Neurotrauma* 21: 9–20.
31. Hopkins, N., E. Cadogan, S. Giles, J. Bannigan, and P. McLoughlin. 2003. Type 2 nitric oxide synthase and protein nitration in chronic lung infection. *J. Pathol.* 199: 122–129.
32. Castegna, A., V. Thongboonkerd, J. B. Klein, B. Lynn, W. R. Markesbery, and D. A. Butterfield. 2003. Proteomic identification of nitrated proteins in Alzheimer's disease brain. *J. Neurochem.* 85: 1394–1401.
33. Greenacre, S. A., and H. Ischiropoulos. 2001. Tyrosine nitration: localisation, quantification, consequences for protein function and signal transduction. *Free Radic. Res.* 34: 541–581.
34. Daubener, W., V. Posdziech, U. Hadding, and C. R. MacKenzie. 1999. Inducible anti-parasitic effector mechanisms in human uroepithelial cells: tryptophan degradation vs. NO production. *Med. Microbiol. Immunol.* 187: 143–147.
35. Swintek, A. U., S. Christoph, F. Petrat, H. de Groot, and M. Kirsch. 2004. Cell type-dependent release of nitric oxide and/or reactive nitrogen oxide species from intracellular SIN-1: effects on cellular NAD(P)H. *J. Biol. Chem.* 279: 639–648.
36. Martin-Romero, F. J., Y. Gutierrez-Martin, F. Henao, and C. Gutierrez-Merino. 2004. Fluorescence measurements of steady state peroxynitrite production upon SIN-1 decomposition: NADH versus dihydrodichlorofluorescein and dihydrohodamine 123. *J. Fluoresc.* 14: 17–23.
37. Aitken, J. B., S. E. Thomas, R. Stocker, S. R. Thomas, O. Takikawa, R. S. Armstrong, and P. A. Lay. 2004. Determination of the nature of the heme environment in nitrosyl indoleamine 2,3-dioxygenase using multiple-scattering analyses of x-ray absorption fine structure. *Biochemistry* 43: 4892–4898.
38. Kurozumi, R., S. Tokuzumi, and S. Kojima. 2003. Does peroxynitrite involve in the elevation of cellular glutathione induced by sodium nitroprusside (SNP) in RAW 264.7 cells? *Biol. Pharm. Bull.* 26: 1070–1075.
39. Mehta, T. R., and R. Dawson, Jr. 2001. Taurine is a weak scavenger of peroxynitrite and does not attenuate sodium nitroprusside toxicity to cells in culture. *Amino Acids* 20: 419–433.
40. Munn, D. H., M. Zhou, J. T. Attwood, I. Bondarev, S. J. Conway, B. Marshall, C. Brown, and A. L. Mellor. 1998. Prevention of allogeneic fetal rejection by tryptophan catabolism. *Science* 281: 1191–1193.
41. Gonzalez, A., A. S. Lopez, E. Alegre, J. L. Alcazar, and N. Lopez-Moratalla. 2004. Does nitric oxide play a role in maternal tolerance towards the foetus? *J. Physiol. Biochem.* 60: 227–238.
42. Brito, C., M. Naviliat, A. C. Tiscornia, F. Vuillier, G. Gualco, G. Dighiero, R. Radi, and A. M. Cayota. 1999. Peroxynitrite inhibits T lymphocyte activation and proliferation by promoting impairment of tyrosine phosphorylation and peroxynitrite-driven apoptotic death. *J. Immunol.* 162: 3356–3366.
43. Kusmartsev, S. A., Y. Li, and S. H. Chen. 2000. Gr-1<sup>+</sup> myeloid cells derived from tumor-bearing mice inhibit primary T cell activation induced through CD3/CD28 costimulation. *J. Immunol.* 165: 779–785.
44. Kuhn, D. M., and T. J. Geddes. 1999. Peroxynitrite inactivates tryptophan hydroxylase via sulfhydryl oxidation: coincident nitration of enzyme tyrosyl residues has minimal impact on catalytic activity. *J. Biol. Chem.* 274: 29726–29732.
45. Kuhn, D. M., M. Sadidi, X. Liu, C. Kreipke, T. Geddes, C. Borges, and J. T. Watson. 2002. Peroxynitrite-induced nitration of tyrosine hydroxylase: identification of tyrosines 423, 428, and 432 as sites of modification by matrix-assisted laser desorption ionization time-of-flight mass spectrometry and tyrosine-scanning mutagenesis. *J. Biol. Chem.* 277: 14336–14342.